Carbon Monoxide Adsorption on Selected Gold Clusters: Highly Size-Dependent Activity and Saturation Compositions

ARTICLE *in* THE JOURNAL OF PHYSICAL CHEMISTRY B · NOVEMBER 2000

Impact Factor: 3.3 · DOI: 10.1021/jp002889b

Carbon Monoxide Adsorption on Selected Gold Clusters: Highly Size-Dependent Activity and Saturation Compositions

William T. Wallace and Robert L. Whetten*

Schools of Chemistry and Physics, Georgia Institute of Technology, Atlanta, Georgia 30332-0430

Received: August 10, 2000; In Final Form: October 2, 2000

The carbon monoxide (CO) adsorption activity of small gold-cluster anions (Au_N^-, $N = 4-19$) has been measured by pulsed helium flow-reactor methods at room temperature. In contrast to other metals, the reaction-product distributions, $Au_N(CO)_M = (N,M)$, measured over a range of CO partial pressure, reveal highly size-dependent adsorption activity and saturation. Preferred initial products include the (N,M) set {(5,1), (11,1), (15,1), (15,2)}, which can be explained by the gold electron (sub)shell fillings at 8, 14, 18, and 20 electrons, respectively, assuming CO acts as a two-electron donor. Pronounced saturation compositions include the complexes {(7,4), (9,6), (11,6), (13,6)}. The pressure-dependent adsorption patterns give insight into (CO,O_2) coadsorption phenomena on model-catalyst systems, and may be exploited in further gas-phase experiments on coadsorption and catalytic cycles.

I. Introduction

The adsorption of carbon monoxide (CO) on gold is cited[1] as the most extensively investigated chemisorption process involving that metal, even though it is characterized by a vanishing sticking probability on extended surfaces at room temperature. The interaction energy is only ∼55 kJ/mol, even on the regularly stepped (332) surface at low coverage.[2] There nonetheless exist compelling reasons to explore it further, particularly with regard to establishing how the CO adsorption parameters depend on the size, structure, and electronic state of nanoparticulate gold substrates. The presently described investigation of CO adsorption processes of gas-phase, negative-charged gold clusters, denoted by

$$Au_N^{(-)} + MCO = Au_N(CO)_M^{(-)} = (N,M,-) \qquad (1)$$

is motivated by the following considerations:

1. Low-Temperature Catalytic Transformations. Interest worldwide has been attracted to the discovery,[3] from the laboratory of Haruta in Osaka,[4] of a family of gold-based catalysts that facilitate a vast class of oxygen-atom transfer reactions at reduced temperatures and with moisture tolerance. Among these are a class of C1 transformations (or their reverse reactions) of special scientific and technical significance:

$CO + (^1/_2)O_2 = CO_2$	combustion
$CO + NO = CO_2 + (^1/_2)N_2$	NO_x reduction
$CO + H_2O = CO_2 + H_2$	water−gas shift
$CO_x + 2H_2 = CH_3OH$	methanol synthesis

Supported gold catalysts have been demonstrated, for each of these, that are comparable to the existing standards in activity, but with a reduced operating temperature and/or effective activation energy (temperature dependence).[1,5] Structurally, such catalysts are quite inhomogeneous systems, but their activity is found to depend critically on the (mean) size of the supported particles or clusters. In one case the dominant particle has been deduced to contain as few as ∼13 atoms,[6] while model catalysts (gold particles on single-crystal substrates) have been described that appear to show optimal activity near 100 atoms,[7] or in the 8−20-atom range.[8,9] There is evidence that the clusters are immobilized at surface oxide vacancies; these common defects comprise localized electrons that could be transferred to the highly electronegative gold clusters bound at those sites.[8] Hence the proposed emphasis on *negatively* charged gold clusters, $Au_N^{(-)}$, or their promoted variants, e.g., neutral KAu_N. New adsorption measurements on such clusters, recorded over a wide range of CO partial pressures, could be valuable for interpreting the transient and steady-state coverages of the supported clusers.

2. Previous Gold-Cluster Investigations. Gold clusters spanning this size range have been variously investigated in the gas phase (or cluster beams),[10] on supports,[11] and as discrete cluster−adsorbate compounds (passivated forms, involving typically PR_3 or RSSR adsorbates).[12,13] (Also, a highly active homogeneous catalyst, the $[M(AuPPh_3)_8]^{2+}$ complex (M = Pd or Pt), has been extensively explored, and its CO adsorbate complex has been structurally characterized.[14]) In the gas phase, attention has been directed to electronic properties, which vary regularly with cluster size and charge, in a manner consistent with an electron-shell model.[15] Chemically, Cox et al.[16] first reported that the room-temperature adsorption (or activation) of H_2, CH_4, and O_2 depends critically on cluster size (N) and charge state (±). In contrast to this, a subsequent brief report[17] mentioned that the initial CO adsorption reactivity on positively charged gold clusters depends only weakly on cluster size, although the complexes Au_7CO^+ and $Au_{19}CO^+$ showed relatively greater resistance to fragmentation. More recently, Lee and Ervin[18] measured the rate of initial CO adsorption on Au_N^- ($N = 2-7$), using low-pressure continuous-flow reactor methods, and reported a rate increasing monotonically with cluster size. Only Au_7^- appeared to approach the high-pressure limit of bimolecular reactions, and the limited pressure range precluded determination of the saturation coverages.

3. Electronic Selection Rules for Chemisorption and Saturation. We have recently established, for the O_2:Au_N^- ($N = 2-22$) adsorption system, a binary-like adsorption behavior (either zero or one molecules adsorbed, at saturation).[19] This is explained by assuming that O_2 acts exclusively as a *one-electron acceptor*, in both the adsorption process and as bound, while

* E-mail: whetten@chemistry.gatech.edu.

10.1021/jp002889b CCC: $19.00
Published on Web 11/04/2000

the gold-cluster subsystem acts to pair its electrons or fill electron shells. Such electron-count driven reactivity is unusual, and raises the question whether it will dominate CO adsorption, i.e., with CO acting as a *two-electron donor*.[20] In the case of the above-mentioned cation experiments,[17] the complexes (7,1,+) and (19,1,+) would then represent the 8- and 20-electron shell closings, since each (neutral) gold atom contributes one electron.

4. Gas-Phase Catalytic Cycles and Enhanced Structural Diagnostics. Gas-phase catalytic chemistry involves sequential or competitive coadsorption processes (e.g., of CO and O_2), as well as elimination of products (CO_2).[21] A separate determination of the pressure-dependent coverage of each reactant is required to perform coadsorption experiments that could mimic the reaction processes occurring on the supported-gold catalysts. In a technical advance of great significance for such experiments, electron diffraction on mass-selected clusters has recently been demonstrated,[22] and could be applied to determine the structural characteristics of the gold subsystem at each stage of CO adsorption (and reaction). Furthermore, many states of CO chemisorption are known (atop, bridge, and hollow sites, as well as various reacted forms), and vibrational spectroscopy (infrared absorption−dissociation, performed on the mass-selected cluster beam) could distinguish among these.[23] An attraction of performing such benchmark adsorption and catalysis experiments is their recently demonstrated theoretical accessibility via first-principles methods.[24]

In this report, we describe experiments which address the questions raised in points 1−3 above, and may also lead toward the experiments 4.

II. Experimental Section

The CO adsorption activity and saturation of gold-cluster anions are measured using a pulsed helium flow reactor (PFR) and detection by time-of-flight mass spectrometry (TOFMS). The method and instrument have been described in detail previously,[19,25] so only a brief summary of its performance characteristics is given here. The gold clusters, charged as well as neutral, are produced by laser ablation of a target rod, entrained and cooled in a pulsed helium nozzle, and then enter the PFR where they merge with a pulsed reactant-gas mixture (dilute CO/He) for a reaction time defined by the length of the reactor channel. At the end of the channel, the merged gas pulses spray into vacuum, are collimated by a slit skimmer, and enter the extraction-field region of the TOFMS, which is set to collect negatively charged clusters of a specified mass range. The reaction conditions are defined by the transit time and by the total and partial pressures in the flow reactor. These are determined by the stagnation pressure behind the primary (gold cluster) and secondary (reactant mixture) pulsed valves (ca. 5 and 1.5 atm, respectively), the relative durations of the gas pulses, and the reactor dimensions (a cylinder 25 mm long by 6 mm diameter, tapering to 3 mm at the exit aperture). A reactor transit time slightly below 100 μs is estimated from the measured timing delays and jet velocities. The small diameter and taper of the reactor yield higher pressures than do other designs.[26]

Time-of-flight mass spectra are accumulated over 1000 waveforms (pulses) and are converted to mass using internal calibration. Assignments of cluster−adsorbate compositions are identified within ±1 amu, and are reproduced in multiple mass spectra.

To access the full range of adsorption phenomena, the composition of the CO/He mixture was varied from below 1% to 20%, and CO was alternatively introduced directly into the primary gas pulse, as described previously for adsorption of O_2.[19] Generally, only relative reactivities or equilibrium constants can be obtained, because the partial pressure of CO actually present in the reactor is not measured. However, for the intial reactivity results one can use the absolute bimolecular rate constant measured by Lee and Ervin[18] for the room-temperature reaction $Au_7^- + CO = Au_7CO^-$, which has a ~5 Å^2 reaction cross-section as the high-pressure limit is approached. Using this reaction as an internal reference, one calculates, for the experiments described below, a CO partial-pressure range of approximately 0.01−0.2 Torr. Alternatively, when a 1% CO/He mixture is used in the primary valve, one can estimate (scaling by cross-sectional area) the CO reactor pressure to be as high as 1 Torr. In either case, the total helium pressure is estimated similarly to approach 100 Torr in the reactor, yielding ~1 ns between buffer gas collisions for Au_7.

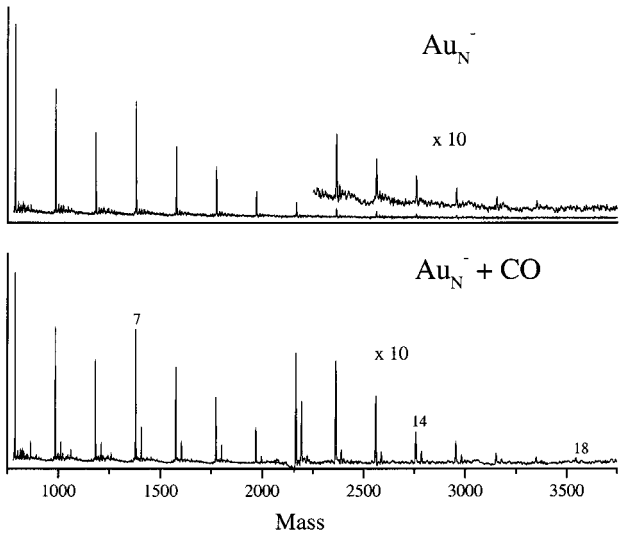

Figure 1. Mass spectra of gold cluster anions, without (upper) and with (lower) exposure to a low dose of CO in the flow reactor.

III. Results

The initial adsorption activity of the gold-cluster anions is assessed at low CO partial-pressure conditions, with the reactant gas introduced by the secondary (downstream) valve. Figure 1 shows typical mass spectra used to calculate product distributions. When the secondary (reactant) gas pulse is displaced temporally from the primary (clusters) pulse, only the clean gold clusters Au_N^- are detected, at the regular mass interval of 197 amu. Overlapping the gas pulses results in the appearance of additional satellite peaks, each displaced M multiples of 28 amu from each principal peak, and assigned to the compositions $Au_N(CO)_M = (N,M)$. As the CO dose is increased (Figure 2), additional satellite peaks (higher M values) appear, and the principal peak becomes relatively weaker. The summed intensity of a principal peak, $I_{N,0}$, and its satellites, $I_{N,M}$, appears to be well conserved over the whole lower range of CO partial pressures. This indicates adsorption-induced cluster fragmentation is not important in this system, just as would have been expected from the low bond energy estimates.[8,18,24] Such pressure-dependent product distributions are used to calculate activity patterns, for each cluster size, in the next section.

Secondary adsorption activity, along with the complete depletion of the principal (N,0) peak, is illustrated by Figure 2A,B, which shows mass spectra obtained using higher CO doses, either by (A) increasing the CO partial pressure in the secondary pulse (intermediate case), or by (B) introducing CO

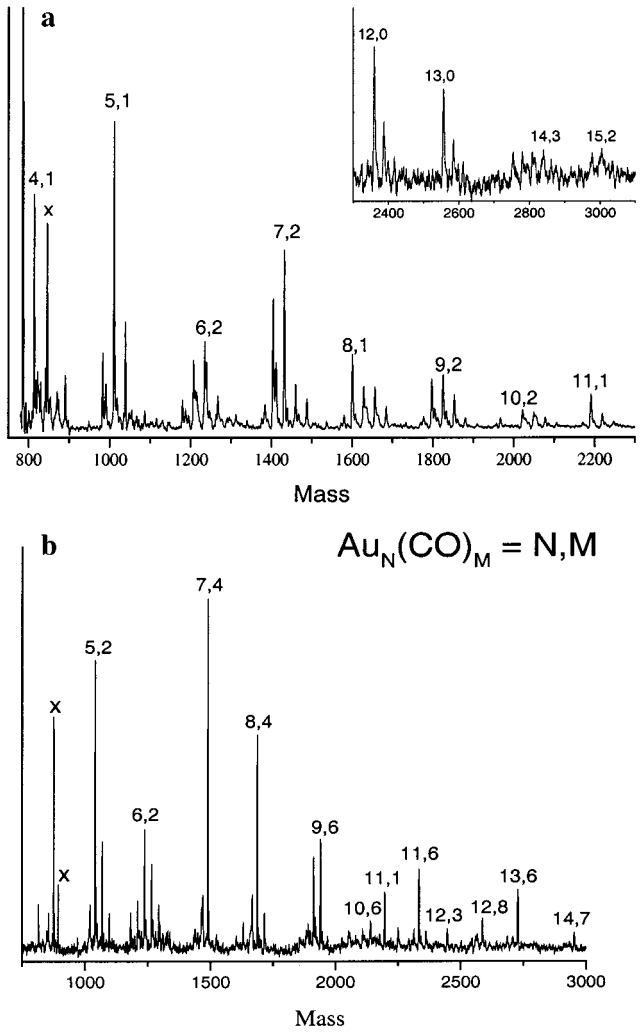

Figure 2. Mass spectra, as in Figure 1, but now under (A) intermediate and (B) high exposure conditions. The new satellite peaks (marked by X) for the $N = 4$ cluster result from trace contamination by O_2; i.e., they are CO_3 (60 amu) and C_2O_4 (88 amu).

directly into the primary gas pulse (high-dose case). [Under these conditions, the time-of-flight mass spectra are complicated by a minor peak emerging between each successive *M*-satellite peak; these features arise from CO desorption occurring in the first field-free flight region of the reflectron mass spectrometer, as verified by reducing the reflecting electric field until such metastable decay products are preferentially detected. See Supporting Information Figure S1.]

Under *intermediate* conditions, Figure 2A, interesting new product distribution patterns emerge. In certain cases (e.g., $N = 6$, 8, 10), the distribution appears unusually flat, with comparable intensities among a range of satellite peaks, as contrasted with the statistical expectation (binomial distribution). In other cases, it is exceptionally peaked, most notably at (5,1), (11,1), (15,1) and (15,2); these "special compositions" are collected in the Table 1.

At the higher doses of Figure 2B, as well as in similar experiments (not shown), evidence of saturation is obtained for many cluster sizes (*N*), where one or two (*N*,*M*) compositions predominate and the patterns become stable with respect to variations in CO dose. (No saturation composition could be determined for Au_4^-, because it is so susceptible to reaction with trace O_2 contamination.) Examples of such saturation peaks are labeled in the illustration, and the saturation compositions (N,M_{max}) are collected in the table.

TABLE 1

A. Special Compositions, $Au_N(CO)_M^{(\pm)} = (N,M,\pm)$ and Electron Counts[a]

$(N,M,\pm)$	N_e	configuration	source
(5,1,−)	8	$1S^2\ 1P^6$	this work
(7,1,+)	8	$1S^2\ 1P^6$	ref 17
(11,1,−)	14	$1S^2\ 1P^6\ (t_{2g})^6$	this work[b]
(15,1,−)	18	$1S^2\ 1P^6\ 1D^{10}$	this work
(15,2,−)	20	$1S^2\ 1P^6\ 1D^{10}\ 2S^2$	this work
(19,1,+)	20	$1S^2\ 1P^6\ 1D^{10}\ 2S^2$	ref 17

B. Saturation Compositions (N,M_{max})

N	M_{max}	other M[b]	$M_{max}(O_2)$[c]	N	M_{max}	other M[b]	$M_{max}(O_2)$[c]
4		1	1	10	6		1
5	4	1−3	0	11	6	1	0
6	4	0−3	1	12	8	3	0,1
7	4		0	13	6		0
8	5	4	1	14	7		1
9	6	5	0				

[a] Electron counts N_e are from eq 4. Configuration expressions, for filled shells, are explained in ref 10. Octahedral symmetry can account for the 14-electron subshell. [b] Other compositions still prominent at conditions approaching saturation. [c] Reference 19.

IV. Analysis and Discussion

A. Initial Adsorption Activity; Kinetic and Equilibrium Analysis. The size-dependent adsorption activity, defined by eq 1, of an *N* series of clusters can be described quantitatively with the aid of a few simple calculations. First, the peak intensities $I_{N,M}$ within each pattern are normalized, so that they can be expressed as (fractional) abundances,

$$f_{N,M} = I_{N,M}/\Sigma_M I_{N,M}$$

where the sum runs from $M = 0$ (the unreacted cluster) to M_{max} (the saturation adsorption). [The $f_{N,M}$ patterns appear identical to the mass spectra, except that each size N now has an equal weight.] Then, assuming kinetic control of the adsorption (i.e., irreversible sequential adsorption steps), the reactivity R_N can be defined in terms of the depletion of the unreacted cluster abundance,

$$R_N = -\log_e [f_{N,M=0}] \qquad (2)$$

Figure 3 combines several examples of R_N plots, constructed from mass spectra obtained at varying CO doses, where in each case the actual R_N values have been normalized to that of R_7, i.e., to the reactivity of Au_7^-,

$$R_N^* = R_N/R_7 \qquad (2^*)$$

Such relative reactivity values should not depend on the CO dose used, again assuming kinetic control. The adsorption rate constant, or equivalently (for initial adsorption in the high-pressure limit) the cross-section, can then be placed on an absolute scale, using the value of ~5 Å^2 obtained in ref 18 for $Au_7^- + CO = Au_7CO^-$.

However, it is more often the case with simple adsorption processes (defined by a negligible barrier to adsorption and no metastable precursor states) that the reaction processes (1) are under equilibrium control. In this case, the appropriate measure of initial activity is the adsorption free energy, expressed by the logarithm of the stepwise equilibrium constant $K_{N,M=0,1}$,

$$\log_e K_{N,M=0,1} = \log_e\{[CO]\, f_{N,M=1}/f_{N,M=0}\} \qquad (3)$$

where [CO] is the partial pressure of carbon monoxide, which

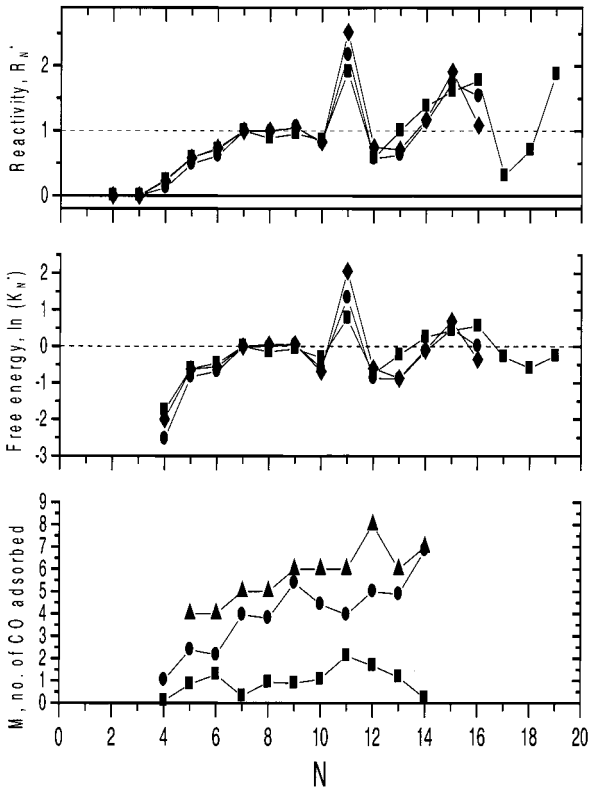

Figure 3. Quantitative analysis of the relative adsorption activity of gold clusters. Size (N) variations in (A) the relative (initial) reactivity, R_N*, as defined in eqs 2 and 2*, where the three data sets correspond to varying CO doses, in the order of squares (lowest, as in Figure 1A), then circles, and finally diamonds; (B) the relative first equilibrium constants, $\log_e(K_N^*)$, eqs 3 and 3*; and (C) the mean (circles) and standard deviation (squares) of the product distribution (M), calculated for the high-dose conditions of Figure 2B. The triangles indicate the highest-M product observed.

may be removed by normalizing to that of K_7, the equilibrium constant for Au_7^-,

$$K_N^* = K_N/K_7 \qquad (3^*)$$

Again, such relative adsorption free-energy values should be invariant to the CO dose used, assuming equilibrium control. (The quantities (3) can be expressed in energy units by multiplying by the factor $k_BT \sim 0.025$ eV corresponding to room temperature.)

The main features of the results collected in Figure 3 can be summarized as follows: (i) No definite indication of room-temperature adsorption activity could be detected for the dimer or trimer; under the saturation conditions of Figure 2B, the corresponding mass range shows only peaks that could not be assigned to any (N,M) combinations. (ii) $N = 4$ is the smallest cluster anion to undergo significant CO adsorption at room temperature; the most reliable estimate places it as no more than $\sim$ 10% as active as Au_7^-. (iii) There is a large step up at Au_5^-, which adsorbs CO readily, i.e., ca. 50−60% as much as Au_7^-; at least part of this high initial activity may be attributed to the special stability of the Au_5CO^- product, as suggested by its reluctance to undergo further CO adsorption. (iv) The activity in the $N = 6-10$ range varies within a narrow band, with a weakly superimposed trend toward an even−odd alteration, with odd-N (even electron count) clusters more active than their neighboring even-N (odd electron count) clusters.[27] (v) $N = 11$ is another special case where the activity jumps to a high value, in this case more than twice that of Au_7^-; of larger clusters, only $N = 15$ consistently approaches that activity level, and several of the larger clusters ($N = 12$, 13, 17) are consistently below $N = 7$. (vi) The present results are insufficient to decide between kinetic and equilibrium limits.

The size range considered here is evidently too narrow for one to draw any conclusion regarding the approach to bulk surfaces, with their vanishing sticking probability at room temperature. Yet it is certainly sufficient to conclude that the adsorption probability fails to continue to rise with increasing size. (The collision cross-section varies little across this size range, since the increase in the cluster's geometrical cross-section, which nearly doubles on going from $N = 7$ to $N = 20$, is largely canceled by the enhanced long-range ion−dipole interaction for smaller clusters.[18])

B. Coverage Patterns and Approach to Saturation. There is clear evidence, in the patterns shown in Figure 2, that subsequent adsorption steps are even more selective with respect to cluster size than is the initial adsorption process. Without evaluating these trends quantitatively, one may yet conclude that: (i) $N = 5$ and 11 are relatively reluctant to adsorb a second CO molecule, while $N = 15$ acts similarly against the third adsorption. (ii) Approaching saturation, there is a pronounced odd−even alternation across the $N = 6-13$ range, as "evens" remain partially unsaturated while "odds" rush toward saturation values. The latter effect may be appreciated by considering the size dependences of the mean coverage and especially its standard deviation, Figure 3C. This behavior is very far indeed from that of a "structure-insensitive reaction", as CO adsorption has often been described.[18,26]

C. Special Compositions and Electron Counting. The table presents all those compositions that have been identified as having enhanced stability, either with respect to their accumulation as intermediate products or as the observed saturated compositions. Also listed is the metal subsystem's valence (or conduction) electron count[10,12] for each of these compositions, namely

$$N_e = (N + 1) + 2M \qquad (4)$$

where the negatively charged gold cluster contributes the parenthetic quantity, and it is assumed, following convention, that CO acts exclusively as a two-electron donor. It is seen that the special intermediate compositions identified can each be explained in terms of the known stability of the 8, 14, 18, and 20 electron shell fillings. (The 19-electron complex (12,3) might also be similarly explained, as a particularly stable odd-electron complex.) However, to consititute a sufficient explanation of the entire pattern, one would also need to find additional special compositions, e.g., (9,2), (13,2), (13,3).

The propensity for even-M values in the saturation composition table raises the further question, whether the CO groups, as adsorbed on gold clusters, might not actually be paired, e.g., as glyoxylate adsorbates, −C(=O)−C(=O)−, in which case only a single electron is donated per CO adsorbed. The saturation compositions (11,6,−) and (13,6,−) could then coincide with 18- and 20-electron shell closings, respectively.

Regardless of the physical basis of the saturation coverages—whether they lie in the number of structural "active sites" or in electron counting—the most obvious conclusion to be drawn is that they are far below the "geometrical" expectation. We anticipate that they may appear implausibly low, particularly as compared with the familiar geometrical saturation achieved by platinum-group metals, consider, e.g., $Ni_{38}(CO)_{36}$[28] or $Pt_{38}(CO)_{44}$.[29] Consider, however, that (i) No such cluster compounds are known for the (Cu,Ag,Au)-group metals; (ii) It is well

established from surface-science investigations[2] that Au (and Cu) surfaces saturate at low CO coverage, even at low temperature, e.g., at ~30 Å^2 per CO ($\theta = 0.17$ fraction of the geometrical coverage) to $T \sim 140$ K, and about twice that area for CO bound to 185 K. Such high areas-per-adsorbate (low fractional coverages), although never explained, are thus intrinsic to metallic gold surfaces, and are more consistent with the saturation values presented here. (A pertinent comparison has been drawn by Cox et al.[16] for the case of H_2 (and CH_4) saturation chemisorption on gold versus other transition-metal clusters.[30])

D. Concluding Remarks. The pressure-dependent adsorption patterns reported here, combined with the previously reported parameters of the O_2:Au cluster system,[19] may help lead to an improved understanding of the technical performance of supported-gold catalysts,[1,4,5] as well as of the sophisticated model-catalyst investigations[7−9] motivated by them. Such experiments variously involve measurements of catalytic activity vs temperature and pressure, under steady-state or cycling dose conditions, as well as IR spectroscopy of the CO-related adsorbate groups at or near saturation. Analogous experiments on unsupported clusters may be revealing, particularly when one considers that the precise role of the support, which might function minimally just to maintain the clusters exposed in a high-activity dispersed state, is often uncertain and highly controversial. For example, it has been argued that successful supported-metal catalysts, e.g., for CO hydrogenation,[31] actually function with submerged metal nano-electrodes, so that their surface chemisorption properties are irrelevant.

The combination of the O_2 binary rule[19] (none or one adsorbed at a time, for each cluster) and the limitations placed here on CO adsorption has interesting consequences that may survive "translation" to the case of the supported clusters. More generally, the electron-counting interpretations above are consistent with the idea[7] that specific, global electronic-structure characteristics may be as important as local (site-specific) structural characteristics in determining the activity of individual particles. The geometrical unsaturation documented here could be significant in allowing for coadsorption and activation of other molecules, such as O_2, NO, H_2, H_2O. Preliminary results on such coadsorption have already been obtained, and will be presented in a forthcoming full report.

Acknowledgment. This research has benefited from stimulating discussions with U. Landman, H. Hakkinen, M. A. El-Sayed, and W. A. deHeer; from technical assistance from B. E. Salisbury; and from financial support from the U.S. National Science Foundation.

Supporting Information Available: Figure identifying metastable decay processes (CO desportion in the first field-free flight region). This material is available free of charge via the Internet at http://pubs.acs.org.

References and Notes

(1) Bond, G. C.; Thompson, D. J. Catalysis by Gold. *Catal. Rev. Sci. Eng*. **1999**, *41*, 319−388.

(2) Ruggiero, C.; Hollins, P. Adsorption of carbon monoxide on the gold (332) surface. *J. Chem. Soc., Faraday Trans.* **1996**, *92*, 4829−4834.

(3) Haruta, M.; Yamada, N.; Kobayashi, T.; Iijima, S. Gold catalysts prepared by coprecipitation for low-temperature oxidation of hydrogen and of carbon monoxide. *J. Catal*. **1989**, *115*, 301. See, for example: Abelson, P. H.; *Science* **2000**, *288*, 269.

(4) The Abilities and Potential of Gold as a Catalyst. Report of the Research Achievements of Interdisciplinary Basic Research section (April 1994−March 1999), Osaka National Research Institute (ONRI) Report No. 393, 1999.

(5) For review, see: Haruta, M. Size- and support-dependency in the catalysis of gold. *Catal. Today* **1997**, *36*, 153−166.

(6) Cunningham, D. A. H.; Vogel, W.; Kageyama, H.; Tsubota, S.; Haruta, M. The relationship between the structure and activity of nm-size gold when supported on $Mg(OH)_2$. *J. Catal*. **1998**, *177*, 1−10.

(7) Valden, M.; Lai, X.; Goodman, D. W. .Onset of Catalytic Activity of Gold Clusters on Titania with the Appearance of Nonmetallic Properties. *Science* **1998**, *281*, 1647−1650.

(8) Sanchez, A.; Abbet, S.; Heiz, U.; et al. When Gold Is Not Noble: Nanoscale Gold Catalysts. *J. Phys. Chem. A* **1999**, *103* (48), 9573−9578.

(9) Heiz, U.; Sanchez, A.; Abbet, S.; Schneider, W.-D. The reactivity of gold and platinum metals in their cluster phase. *Eur. Phys. J.* **1999**, *D9*, 35−39.

(10) deHeer, W. A. The physics of simpler metal clusters: experimental aspects and models. *Rev. Mod. Phys*. **1993**, *65*, 611−676.

(11) Marks, L. D. *Rep. Prog. Phys.* **1994**, *57*, 603−649.

(12) Mingos, D. M. P.; Slee, T.; Zhenyang, L. Bonding models for ligated and bare clusters. *Chem. Rev.* **1990**, *90*, 383−402.

(13) Schaaff, T. G.; Whetten, R. L. Giant gold-glutathione cluster compounds. *J. Phys. Chem.* **2000**, *104*, 2630−2641 and references therein.

(14) Pignolet, L. H. Catalysis by mixed-metal clusters containing gold phosphine couplings. In *Catalysis by di- and polynuclear metal cluster complexes*; Adams, R. D., Cotton, F. A., Eds.; Wiley-VCH: New York, 1998; pp 95−126.

(15) Taylor, K. J. Pettiette-Hall, C. L.; Cheshnovsky, O.; et al. Ultraviolet photoelectron spectra of coinage metal clusters. *J. Chem. Phys*. **1992**, *96* (4), 3319−3329.

(16) Cox, D. M.; Brickman, R.; Creegan, K.; et al. Gold Clusters: reactions and deuterium uptake. *Z. Phys.* **1991**, *D19*, 353−355. Cox, D. M.; Brickman, R. O.; Creegan, K. Studies of the Chemical Properties of Size Selected Metal Clusters: Kinetics and Saturation. *Mater. Res. Soc. Symp. Proc*. **1991**, *206*, 34−48.

(17) Nygren, M. A.; Siegbahn, P. E. M.; Jin, C.-M.; Guo, T.; Smalley, R. E. Electronic shell closings in metal cluster plus adsorbate systems: Cu_7^+-CO and Cu_{17}^+CO. *J. Chem. Phys.* **1991**, *95*, 6181−4.

(18) Lee, T. H.; Ervin, K. M. Reactions of Copper Group Anions with Oxygen and Carbon Monoxide. *J. Phys. Chem*. **1994**, *98* (40), 10023−10031. Lee, T. H. Reactions and Bond Dissociation Energies of Bare and Ligated Copper Group Anions. Dissertation, Unversity of Nevada, Reno, 1995.

(19) Salisbury, B. E.; Wallace, W. T.; Whetten, R. L. Low-temperature activation of molecular oxygen by gold clusters. *Chem. Phys.* **2000**, *262*, 119−120. Salisbury, B. E. PhD dissertation, Georgia Institute of Technology, 1999.

(20) Knickelbein, M. B. Reactions of transition metal clusters with small molecules. *Annu. Rev. Phys. Chem*. **1999**, *50*, 79−115.

(21) Shi, Y.; Ervin, K. M. Catalytic oxidation of carbon monoxide by platinum cluster anions. *J. Chem. Phys*. **1998**, *108*, 1757−1760. See also: Kappes, M. M.; Staley, R. H. *J. Am. Chem. Soc*. **1981**, *103*, 1286.

(22) Maier-Borst, M.; Cameron, D. B.; Rokni, M.; Parks, J. H. Electron diffraction of trapped cluster ions. *Phys. Rev. A59*, **1999**, R3162−3165. Krückeberg, S.; Schooss, D.; Maier-Borst, M.; Parks, J. H. Diffraction of trapped cesium-iodide clusters: the appearance of the bulk structure. *Phys. Rev. Lett.* **2000**, in press.

(23) Boccuzzi, F.; Chiorino, A. FTIR study of CO oxidation on Au/TiO_2. *J. Phys. Chem*. **2000**, *104*, 5414−6 and references therein.

(24) Häkkinen, H.; Landman, U. Gold clusters and their anions. *Phys. Rev. B* **2000**, *62*, R2287−R2290.

(25) Livingston, F. E. Adsorption of atmospheric gases on alkali-halide nanocrystals. Ph. D dissertation, UCLA, 1995. Homer, M. L.; Livingston, F. E.; Whetten, R. L. Molecular adsorption−desorption reactions of ammonia on alkali-halide clusters and nanocrystals. *J. Phys. Chem*. **1995**, *99*, 7604−7612.

(26) Cox, D. M.; Reichmann, K. C.; Trevor, D. J.; Kaldor, A. CO chemisorption on free gas-phase metal clusters. *J. Chem. Phys.* **1987**, *88*, 111−119.

(27) The lower activity of odd-electron clusters may seem counter-intuitive. However, as an anonymous reviewer points out, "As a two-electron donor, CO will have a repulsive interaction with the singly occupied HOMO for even-*N* clusters. Thus the question is the relative energies of the LUMOs for the even and odd clusters."

(28) Parks, E. K.; Nieman, G. C.; Kerns, K. P.; Riley, S. J. Reactions of Ni_{38} with N_2, H_2, and CO. *J. Chem. Phys.* **1997**, *107*, 1861−1871.

(29) Roth, J. D.; Lewis, G. J.; Stafford, L. K.; Jiang, X.; Dahl, L. R.; Weaver, M. J. Exploration of the ionizable metal cluster-electrode surface analogy. *J. Am. Chem. Soc.* **1992**, *114*, 6159−6164.

(30) Cox, D. M.; Fayet, P.; Brickman, R.; Hahn, M. Y.; Kaldor, A. Abnormally large deuterium uptake on small transition-metal clusters. *Catal. Lett.* **1990**, *4*, 271−278.

(31) Frost, J. C. Junction effect interactions in methanol synthesis catalysts. *Nature* **1988**, *334*, 577−580.